Science of the Total Environment 703 (2020) 135041

Contents lists available at ScienceDirect

Science of the Total Environment

journal homepage: www.elsevier.com/locate/scitotenv

Selenium tolerance, accumulation, localization and speciation in a *Cardamine* hyperaccumulator and a non-hyperaccumulator

Eszter Borbála Both [a,b], Gavin C. Stonehouse [b], Leonardo Warzea Lima [b], Sirine C. Fakra [c], Bernadette Aguirre [d], Ami L. Wangeline [d], Jiqian Xiang [e], Hongqing Yin [e], Zsuzsa Jókai [a], Áron Soós [f], Mihály Dernovics [g,*], Elizabeth A.H. Pilon-Smits [b]

[a] Department of Applied Chemistry, Szent István University, Villányi út 29-43., 1118 Budapest, Hungary
[b] Department of Biology, Colorado State University, 251 West Pitkin Street, Fort Collins, CO 80523, USA
[c] Advanced Light Source, Lawrence Berkeley National Lab, 1 Cyclotron Road, Berkeley, CA 94720, USA
[d] Biology Department, Laramie County Community College, 1400 E. College Drive, Cheyenne, WY 82007, USA
[e] Enshi Autonomous Prefecture Academy of Agriculture Sciences, 517 Shizhou Road, Enshi, Hubei Province 445002, China
[f] Institute of Food Science, Faculty of Agricultural and Food Sciences and Environmental Management, University of Debrecen, Böszörményi út 138., 4032 Debrecen, Hungary
[g] Department of Plant Physiology, Agricultural Institute, Centre for Agricultural Research, Hungarian Academy of Sciences, Brunszvik u. 2., 2462 Martonvásár, Hungary

HIGHLIGHTS

- Hyperaccumulator *C. violifolia* was evaluated in comparison with a non-accumulator.
- Se physiology & biochemistry of *C. violifolia* differ from known hyperaccumulators.
- Neither *Cardamine* species showed evidence of growth stimulation by selenium.
- Phosphate didn't inhibit selenite uptake at neither Cardamine species.
- μXANES and LC-ICP-MS data support selenocystine-free Se accumulation.

GRAPHICAL ABSTRACT

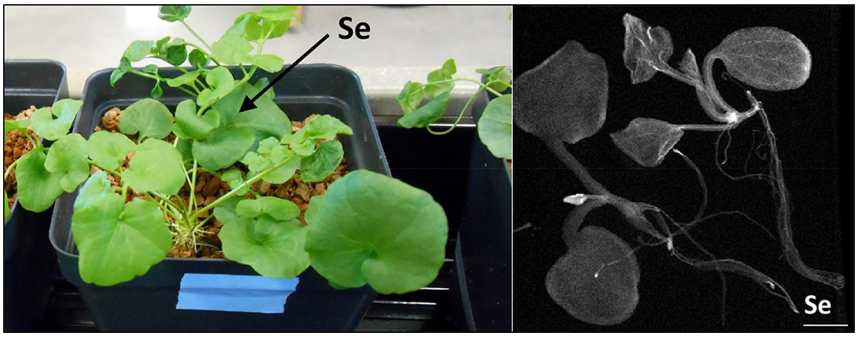

ARTICLE INFO

Article history:
Received 16 August 2019
Received in revised form 16 October 2019
Accepted 16 October 2019
Available online 2 November 2019

Editor: Charlotte Poschenrieder

Keywords:
Cardamine
Hyperaccumulation

ABSTRACT

Cardamine violifolia (family *Brassicaceae*) is the first discovered selenium hyperaccumulator from the genus *Cardamine* with unique properties in terms of selenium accumulation, i.e., high abundance of selenolanthionine. In our study, a fully comprehensive experiment was conducted with the comparison of a non-hyperaccumulator *Cardamine* species, *Cardamine pratensis*, covering growth characteristics, chlorophyll fluorescence, spatial selenium/sulfur distribution patterns through elemental analyses (synchrotron-based X-Ray Fluorescence and ICP-OES) and speciation data through selenium K-edge micro X-ray absorption near-edge structure analysis (μXANES) and strong cation exchange (SCX)-ICP-MS. The results revealed remarkable differences in contrast to other selenium hyperaccumulators as neither *Cardamine* species showed evidence of growth stimulation by selenium. Also, selenite uptake was not inhibited by phosphate for either of the *Cardamine* species. Sulfate inhibited selenate uptake, but the two *Cardamine* species did not show any difference in this respect. However, μXRF derived speciation

Abbreviations: ALS, Advanced Light Source; Chl, chlorophyll; DW, dry weight; GAE, gallic acid equivalent; HA, hyperaccumulator; HPLC, high performance liquid chromatography; ICP-OES, inductively coupled plasma optical emission spectroscopy; LC-ICP-MS, liquid chromatography inductively coupled plasma mass spectrometry; LOQ, limit of quantification; LSQ, least squares; MALDI-HRMS, matrix assisted laser desorption ionization high resolution mass spectrometry; MS, Murashige and Skoog; ND, non detected; NPQt, non-photochemical quenching; Phi2, quantum yield of Photosystem II (photochemical quenching); PTFE, polytetrafluoroethylene; SCX, strong cation exchange; SEM, standard error of means; SULTR, sulfate transporters; TEAC, Trolox-equivalent antioxidant capacity; μXRF, micro-focused x-ray fluorescence; μXANES, X-ray absorption near-edge structure.

* Corresponding author.
E-mail address: dernovics.mihaly@agrar.mta.hu (M. Dernovics).

https://doi.org/10.1016/j.scitotenv.2019.135041
0048-9697/

Selenium
Selenolanthionine
X-ray microprobe analysis

maps and selenium/sulfur uptake characteristics provided results that are similar to other formerly reported hyperaccumulator and non-hyperaccumulator *Brassicaceae* species. μXANES showed organic selenium, "C-Se-C", in seedlings of both species and also in mature *C. violifolia* plants. In contrast, selenate-supplied mature *C. pratensis* contained approximately half "C-Se-C" and half selenate. SCX-ICP-MS data showed evidence of the lack of selenocystine in any of the *Cardamine* plant extracts. Thus, *C. violifolia* shows clear selenium-related physiological and biochemical differences compared to *C. pratensis* and other selenium hyperaccumulators.

1. Introduction

Cardamine violifolia, a selenium (Se) hyperaccumulator (HA) species from the family of *Brassicaceae* and native to seleniferous soils in the Yutangba region in China, has been found earlier to contain a novel major Se species, selenolanthionine (Both et al., 2018). Findings of high Se accumulation in *Cardamine* species from this region in Enshi, China (Shao et al., 2014) have also been published under the names *C. hupingshanesis* (Yuan et al., 2013) and *C. enshiensis* (Cui et al., 2018); these relate to the same Se-tolerant *Cardamine* species to the best of our knowledge. This seleniferous part of China is characterized by soils and water sources with very high Se content (up to 2.4 mg water-soluble Se/kg soil and up to 275 μg Se/L, respectively) (Chang et al., 2019; Fordyce et al., 2000; Qin et al., 2012; Xing et al., 2015; Zhu et al., 2008; Zhu et al., 2004). Values for total Se concentration in *C. violifolia* shoot tissues reported earlier are 1.8–4.4 g Se/kg dry weight (DW), which places this plant in the group of HA (Both et al., 2018; Cui et al., 2018; Yuan et al., 2013).

The Se metabolism and the enzymatic activities involved in its uptake, accumulation and exclusion processes in Se accumulator organisms can be regressively analyzed through the identification of the main or abundant Se species resulted from these processes. As an example, the detection of high amounts of Se-methylselenocysteine inherently assumes the high activity of selenocysteine Se-methyltransferase (Freeman et al., 2010; Sors et al., 2009), while HA containing other organic forms of Se, e.g., selenocystathionine, selenohomolanthionine or selenomethionine (Montes-Bayon et al., 2002; Ogra et al., 2007; Virupaksha and Shrift, 1963), may reflect other tolerance mechanisms.

The completion of chemical speciation data obtained from well-homogenized bulk plant material requires a comprehensive approach. Facing the relatively low molecular weight of Se species (mostly < 300 Da), mass spectrometry based imaging such as with MALDI-HRMS that proved to be highly efficient for, e.g., oligosaccharides and lipids (Sarabia et al., 2018) and flavonoids (Crecelius et al., 2017), hasn't been successfully addressed in this field. X-ray fluorescence offers a powerful option to analyze elemental distribution in intact plant tissues. XRF has already been applied for the determination of spatial distribution of Se and has revealed interesting differences between species, particularly between Se HA and related non-HA (Freeman et al., 2012; Silva et al., 2018). μXANES can provide additional information on Se speciation, i.e., the identification of abundant Se forms. This technique has already been proven to be useful not only to discriminate inorganic and organic Se species but to reveal basic features of the chemical bonds of Se at a spatial resolution of < 1 mm (Banuelos et al., 2011; Cruz-Jimenez et al., 2005; Eiche et al., 2015).

The goal of this study was to provide novel information on the Se-related physiological and biochemical properties of *C. violifolia*, in comparison with a presumably non-hyperaccumulator (non-HA) relative, *Cardamine pratensis L.* (cuckooflower) with a fully comprehensive approach including XRF, XANES, Chl (chlorophyll) fluorescence and LC-ICP-MS (liquid chromatography inductively coupled plasma mass spectrometry) analyses among others. Such deep studies covering the HA and non-HA species of a plant genus has only been conducted in parts for some well-known *Fabaceae* species like *Astragalus* (Statwick et al., 2016) and *Brassicaceae* species (*Stanleya pinnata vs. S. elata*; Lindblom et al. (2014)). Accordingly, the main questions are related to the tolerance of Se accumulation, the physiological responses to Se, as well as the spatial distribution and the chemical species of Se. Beyond the expected differences between the HA and non-HA *Cardamine* species in terms of Se accumulation capacity and Se:S ratio, the Se induced growth stimulation and Se uptake inhibition by sulfate, formerly reported characteristics of primary Se accumulators, were the focus of this study. Special attention was paid to the unambiguous identification of selenocystine, the compound reported to be responsible for the high Se accumulation of HA *Cardamine* species, which could be considered a unique feature among *Brassicaceae* plants.

2. Materials and methods

2.1. Biological materials

Cardamine violifolia leaves, roots and seeds were collected in the Yutangba region and were provided by the Academy of Agricultural Sciences of Enshi Tujia and Miao Autonomous Prefecture (Wuhan, China). *Cardamine pratensis* (cuckooflower) seeds were purchased from Seedaholic (Cloghbrack, Clonbur, Ireland).

2.2. Reagents and standards

Murashige and Skoog (MS) medium, ethanol, sucrose, ammonium nitrate, calcium nitrate tetrahydrate, ethylenediaminetetraacetic acid ferric sodium salt, potassium nitrate, potassium hydroxide, magnesium sulfate heptahydrate, potassium phosphate monobasic, magnesium chloride hexahydrate, boric acid, manganese (II) sulfate monohydrate, zinc sulfate heptahydrate, copper (II) sulfate pentahydrate, molybdenum (VI) oxide, sodium selenate, L-selenocystine, sodium borohydride, sodium selenite, trolox and Folin & Ciocalteu's phenol reagent were obtained from the Merck – Sigma group (St. Louis, MO, USA). Phytoagar was purchased from Research Products International (Mt. Prospect, IL, USA). Pyridine (a. r.) was obtained from Carlo Erba (Peypin, France), while formic acid was purchased from Scharlau (Barcelona, Spain). Standards for ICP-OES calibration were obtained from Elemental Scientific (Omaha, NE, USA).

2.3. Cultivation of plants

2.3.1. Cultivation of plants on sterile media for tolerance and accumulation experiments and for X-ray microprobe analysis

Seeds of *C. violifolia* and *C. pratensis* were surface-sterilized by rinsing consecutively with 70% ethanol (1 min), sterilized distilled water (10 min), 10% household bleach (10 min) and finally five times (10 min each) with sterilized distilled water. After steriliza-

tion, the seeds were incubated in distilled water for two days at 4 °C for stratification. Subsequently, the seeds were germinated on sterilized wet filter paper, before transferring to agar media after the radicle emerged. Half-strength MS agar medium was used, consisting of 2.22 g/L MS basal salt mixture (Murashige and Skoog, 1962), 10 g/L sucrose, 8 g/L Phytoagar, pH 5.6–5.8 (set with KOH), sterilized by heating to 120 °C for 20 min. After the media had cooled to 55 °C, different concentrations of Na_2SeO_4 (0, 50, 100, 200, 400 μM) were added, and square petri dishes (12 × 12 cm) were prepared. After the medium had solidified, germinated seeds were carefully placed on the medium along a line approximately 2 cm from one of the edges, with 1 cm distance (10 seeds per plate). Petri dishes were sealed with a double layer of parafilm and placed vertically in an incubator, with the seeds forming a horizontal line along the top rim of the Petri dishes. Plants were incubated in this manner in a growth cabinet at 23 °C and a 16 h: 8 h (light:dark photoperiod). After 26 days, photos were taken and root lengths were determined from the photos using Image J2 software (Rueden et al., 2017). Plants were then harvested, rinsed in distilled water, separated into shoots and roots and dried at 50 °C for 48 h. Dry weight data of shoots were determined (roots were too small to be weighed accurately), and the shoots from the different selenate treatments were used for elemental analysis as described below.

Essentially the same protocol was used for the preparation of seedlings for X-ray microprobe analysis, total phenolic content and antioxidant capacity analyses, using 25 μM selenate in the agar media. The plates were incubated horizontally for these purposes, and the seeds distributed across the entire surface.

2.3.2. Cultivation of plants on gravel for the Se accumulation study and for Chl fluorescence measurements

Seeds of both species were cold treated in distilled water (two days at 4 °C) and sown in 10 × 10 cm pots filled with washed Turface® (PROFILE Products LLC; Buffalo Grove, IL, USA) growth medium (pH 5.5). Plants were grown at 23 °C and under 10 h: 14 h light:dark photoperiod in a growth room. During germination, the seeds were treated with water, and after germination the seedlings were gradually exposed to nutrients over two weeks: during the first week 1/8th Hoagland's nutrient solution (Hoagland and Arnon, 1950) and during the second week 1/4th strength Hoagland's. In order to investigate the uptake capacity of different forms of Se (selenate, selenite) and the interactions of sulfate and phosphate, five different treatments were then applied for 10 days: (A) 1/4th strength Hoagland's solution control treatment, (B) 1/4th strength Hoagland's solution with 20 μM Na_2SeO_4, (C) 1/4th strength Hoagland's solution with 20 μM Na_2SeO_4 and 5 mM $MgSO_4$, (D) 1/4th strength Hoagland's solution with 20 μM Na_2SeO_3, and (E) 1/4th strength Hoagland's solution with 20 μM Na_2SeO_3 and 2.4 mM KH_2PO_4. After the 10-day long treatments, Chl fluorescence measurements were carried out using a MultispeQ 2.0 instrument (Photosynq LLC, East Lansing, MI, USA) using the company's recommended protocol. Plants were then harvested, rinsed, shoots and roots were separated and dried (50 °C for 48 h) for elemental analysis as described below.

2.3.3. Cultivation of selenium enriched C. pratensis for LC-ICP-MS analysis

Seeds of *C. pratensis* were cold treated in distilled water (two days at 4 °C) and sown in 20 × 10 cm pots filled with sterilized garden soil. The pots were kept at 21 °C and under 16 h: 8 h light:dark photoperiod in a growth room. During germination, the seeds were treated with water, and after germination (day #14) the seedlings were transferred into Vermex vermiculite (Soprema; Strasbourg, France). From day #18 1/16th strength Hoagland's nutrient solution was applied that was increased to 1/8th strength from day #21 and to 1/4th strength from day #28. From day #32, 1/4th strength modified Hoagland's solution including 20 μM Na_2SeO_4 and $MgCl_2$ instead of $MgSO_4$ was applied until harvesting (day #40). Leaves and stems were rinsed, lyophilized and milled.

2.4. Elemental analysis

2.4.1. Inductively coupled plasma optical emission spectrometry

Samples were digested in nitric acid as described by Zarcinas et al. (1987). Inductively coupled plasma optical emission spectrometry (ICP-OES) was used as described by Fassel (1978) to determine Se and S concentrations in the samples using a Perkin Elmer Optima 7000 DV ICP-OES, at 196.026 nm (Se) and 181.975 nm (S), respectively, and using appropriate blanks, standards and quality controls. The limits of quantification for Se and S were ~1 mg/kg and ~0.2 mg/kg DW in plant samples, respectively.

2.4.2. Inductively coupled plasma mass spectrometry

Microwave digestion of the *C. violifolia* leaf and root samples from China and *C. pratensis* biomass was carried out in a CEM Mars-5 digestion system (CEM; Matthews, NC, USA). 50 mg of the samples were mixed with 5.0 ml HNO_3 in PTFE digestion tubes and after 24 h 3.0 ml H_2O_2 was added prior to the microwave digestion process. The pressure was raised to 250 psi over 20 min and held for 15 min. Total Se concentration was determined with an Agilent 7500cs ICP-MS (Agilent Technologies, Santa Clara, CA, USA) on the ^{77}Se and ^{82}Se isotopes by the method of standard addition using rhodium (^{103}Rh) as an internal standard. The limit of quantification for Se was ~0.05 mg/kg DW in plant samples.

2.5. Statistical analysis

Statistical analysis was performed with the IBM SPSS v.20 software (Armonk, NY, USA). Two-way ANOVA model was applied to compare the means of the measured parameters with the factors "species" and "treatment". The normality of residuals and the homogeneity of variances were checked. In case of non-normality, data transformation was carried out. Tukey-Kramer's (Tukey, 1977) or Games-Howell's post hoc test (Games and Howell, 1976) was used, depending on the fulfilment of homogeneity of variances assumption. Student's *t*-test or Welch's *t*-test was applied to compare two means, depending on the fulfilment of homogeneity of variances assumption (Jaccard et al., 1984).

2.6. Preparation of selenolanthionine standard

Selenolanthionine was synthesized as described elsewhere (Both et al., 2018). Preparative chromatographic purification was carried out on a Luna strong cation exchange column (250 mm * 10 mm * 10 μm; Phenomenex, Torrance, CA, USA). Gradient elution was done with pyridine formate (pH 3.55; buffer A: 1 mM; buffer B: 40 mM). The program was as follows: 0–15 min from 0% up to 30% B (2.5 ml/min), 15.1–16 min up to 100% B (2.5 ml/min), 16.1–17 min 100% B (3.0 ml/min), 17.1–17.5 min down to 0% B (3.0 ml/min), 17.6–25.9 min 0% B (3.0 ml/min), 25.9–26 min 0% B (2.5 ml/min). Injection volume was 1 μl. The peak corresponding to selenolanthionine was collected from 20 subsequent runs, pooled and lyophilized. The standard was dissolved in distilled water for recording the XANES spectra.

2.7. Selenium distribution and speciation analysis using X-ray microprobe analysis

Entire *C. violifolia* and *C. pratensis* seedlings grown on agar media containing 25 μM selenate were collected at harvest, rinsed,

flash-frozen in liquid nitrogen and stored at −80 °C. Furthermore, young leaves from the plants grown on Turface® media (treatment "B" and "D", see above) were collected at harvest, flash-frozen and stored at −80 °C. The samples were shipped on dry ice for microprobe analyses. These analyses were performed at beamline 10.3.2 (X-Ray Fluorescence Microprobe) of the Advanced Light Source (ALS), at Lawrence Berkeley National Lab (Berkeley, CA, USA) using a Peltier cooling stage (-25 °C). Selenium, calcium (Ca) and potassium (K) distribution were mapped using micro-focused X-ray fluorescence (μXRF), and Se speciation was investigated using X-ray absorption near-edge structure (μXANES) spectroscopy, essentially as described previously (Jiang et al., 2018). Micro-focused X-ray fluorescence (μXRF) maps were recorded at 13 keV incident energy, using 20 μm × 20 μm pixel size, a beam spot size of 7 μm × 7 μm, using 50 ms dwell time. Maps were then deadtime-corrected and decontaminated. Selenium K-edge micro X-ray absorption near-edge structure (μXANES) spectroscopy (in the range 12500–13070 eV) was used to analyze Se speciation on different spots, close to areas showing high Se concentration in the μXRF maps. Spectra were energy calibrated using a red amorphous Se standard, with the main peak set at 12660 eV. Least-square linear combination fitting of the μXANES data was performed in the range of 12630–12850 eV using a library of 52 standard selenocompounds and procedures described elsewhere (Fakra et al., 2018). All data were recorded in fluorescence mode using a 7-elements Ge solid state detector (Canberra, ON, Canada) and processed using custom LabVIEW programs (National Instruments, Austin, TX, USA) available at the beamline.

2.8. Antioxidant capacity analysis and total phenolic content

Seedlings of *C. violifolia* and *C. pratensis* grown on agar media containing 25 μM selenate or without selenate were harvested and flash frozen. Samples were lyophilized, powdered and weighed. The freeze-dried material was extracted with 80% acetone at a ratio of 25 μl/mg tissue while rotated in the dark at 4 °C for 30 min. Supernatant was collected, diluted with additional acetone at 1:10 or 1:20 depending on the sample, and stored on ice until used. For the antioxidant capacity assay, the absorbancies of the diluted supernatants were recorded at λ = 734 nm with a UV–Vis spectrophotometer (PowerWaveXS2; BioTek Instruments, Winooski, VT) using the method of Miller and Rice-Evans (1996). Trolox (a water-soluble analogue of vitamin E) was used as standard for this assay, and results are expressed as micromoles of trolox-equivalent antioxidant capacity (TEAC) per gram dry weight (μmole TE/g DW). Diluted supernatant collected from extraction described above was used for total phenolics. Folin & Ciocalteu's reagent was used as described by Singleton and Rossi (1965). All samples for this assay were recorded at λ = 765 nm using gallic acid as a standard with results expressed as milligrams of gallic acid equivalent (GAE) per gram of dry weight (mg GAE/g DW).

2.9. Strong cation exchange (SCX) chromatography – ICP-MS analysis

0.5 g of *C. violifolia* leaf and root were extracted with 10 ml deionized water using an ultrasonic probe (UP100H, Hielscher Ultrasound Technology, Teltow, Germany) at ambient temperature. The supernatants were recovered by centrifugation (10 min at 4000*g*) and filtered through 0.45 μm cellulose acetate filters. 2.0 ml of the leaf extract and 3.0 ml of the root extract were lyophilized and redissolved in 2.0 ml deionized water. 0.1 ml sample was diluted with 1.4 ml eluent buffer and 20 μl was injected onto the column. In case of spiking, the samples were spiked to 200 ng/ml selenocystine ($SeCys_2$) concentration (calculated as Se).

The chromatographic set-up consisted of an Agilent 1200 HPLC system connected to the Agilent 7500cs ICP-MS for element-specific detection of ^{77}Se and ^{82}Se. A Zorbax 300-SCX column (150 mm × 4.6 mm × 5 μm, Agilent) was used in gradient elution mode with pyridine formate (pH 2.2; buffer A: 1 mM; buffer B: 40 mM) delivered at 1.2 ml/min. The program was as follows: 0–2 min 0% B, 2–15 min up to 30% B, 15–16 min up to 100% B, 16–20 min 100% B, 20–21 down to 0% B, 21–26 min 0% B.

0.3 g of lyophilized *C. pratensis* biomass was extracted with 10 ml deionized water using a vortex shaking device for 5 min. The supernatant was recovered by centrifugation (10 min at 9000*g*), filtered through 0.45 μm PTFE filters and 20 μl was injected onto the column without any dilution. In case of spiking, the samples were spiked to 500 ng/ml $SeCys_2$ (calculated as Se). The chromatographic set-up consisted of a Thermo Spectra System P4000 HPLC pump (Thermo Fisher Scientific, Waltham, MA, USA) connected to the Thermo Scientific X-Series II ICP-MS for element-specific detection of ^{78}Se and ^{80}Se, using 7% H_2-93% He as collision gas, introduced at 6.0 ml/min. A Luna SCX column (250 mm × 4.6 mm × 10 μm; Phenomenex) was used in gradient elution mode with pyridine formate (pH 3.0; buffer A: 1 mM; buffer B: 40 mM). The program was as follows: 0–1 min 0% B (1.7 ml/min), 1–15 min from 0% up to 30% B (1.7 ml/min), 15–16 min up to 100% B (1.9 ml/min), 16–21 min 100% B (1.9 ml/min), 21–21.5 min down to 0% B (1.7 ml/min), 21.5–26 min 0% B (1.7 ml/min).

3. Results

3.1. Selenium accumulation experiments

Selenium hyperaccumulator (HA) *C. violifolia* and non-HA *C. pratensis* grown on agar media without the addition of selenate showed similar root lengths (Fig. 1A) but differed in shoot dry weight (DW), which was 3.5-fold smaller for *C. pratensis* (Fig. 1B),

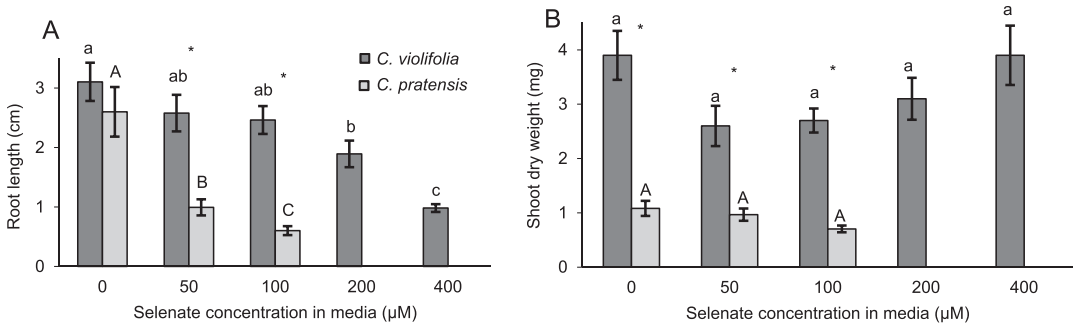

Fig. 1. Root length (A) and shoot biomass (B) of *C. violifolia* (Se hyperaccumulator) and *C. pratensis* (control) grown on agar media supplied with different concentrations of Na_2SeO_4. Values shown are the means ± SEM. Different letters indicate statistically different means among treatments within species (P < 0.05). Asterisks indicate statistically different means between species within treatments (P < 0.05). Note: there was no germination for *C. pratensis* on 200 and 400 μM Se.

likely reflecting different plant species characteristics. The effect of selenate on root growth was more pronounced for *C. pratensis*: its 50% inhibition point was below 50 μM selenate and its highest tolerated Se concentration was 100 μM selenate, a concentration at which *C. violifolia* was still unaffected (Fig. 1A). *C. violifolia* root length was 50% inhibited between 200 and 400 μM selenate (Fig. 1A). Shoot dry weight was not significantly inhibited by Se in either species (Fig. 1B). Overall it can be concluded that the HA *C. violifolia* is relatively more tolerant to selenate than the non-HA *C. pratensis*.

At 50 μM selenate, seedlings of both species accumulated around 1000 mg Se/kg DW in shoots (Fig. 2A). However, at 100 and 200 μM selenate, Se accumulation in HA *C. violifolia* reached 2000 and 2700 mg Se/kg DW, respectively, while in *C. pratensis* the Se concentration was below 500 mg/kg DW at the 100 μM treatment, and the plants did not survive the higher Se treatments. *C. violifolia* Se levels were around 1000 mg/kg DW at the 400 μM treatment, similar to that obtained for the 50 μM treatment (Fig. 2A). Se:S molar ratio in *C. violifolia* shoot increased with increasing selenate supplied. At 400 μM treatment the Se:S ratio was the same compared to 200 μM, despite the lower Se concentration (Fig. 2B). As a result, *C. violifolia* showed an increasing shoot S concentration pattern according to the higher selenate supply up to 100 μM; in contrast, *C. pratensis* showed an opposite pattern, decreasing the S concentration with higher selenate supply (Fig. 2C). It can be concluded that *C. violifolia* is capable of higher Se accumulation than *C. pratensis*. Furthermore, *C. pratensis* is also capable of reaching significant tissue Se levels, however, the accumulation breaks down at elevated selenate concentrations, which is an indicative of a lack of Se tolerance. Additionally, Se-S interactions differ between the HA and non-HA.

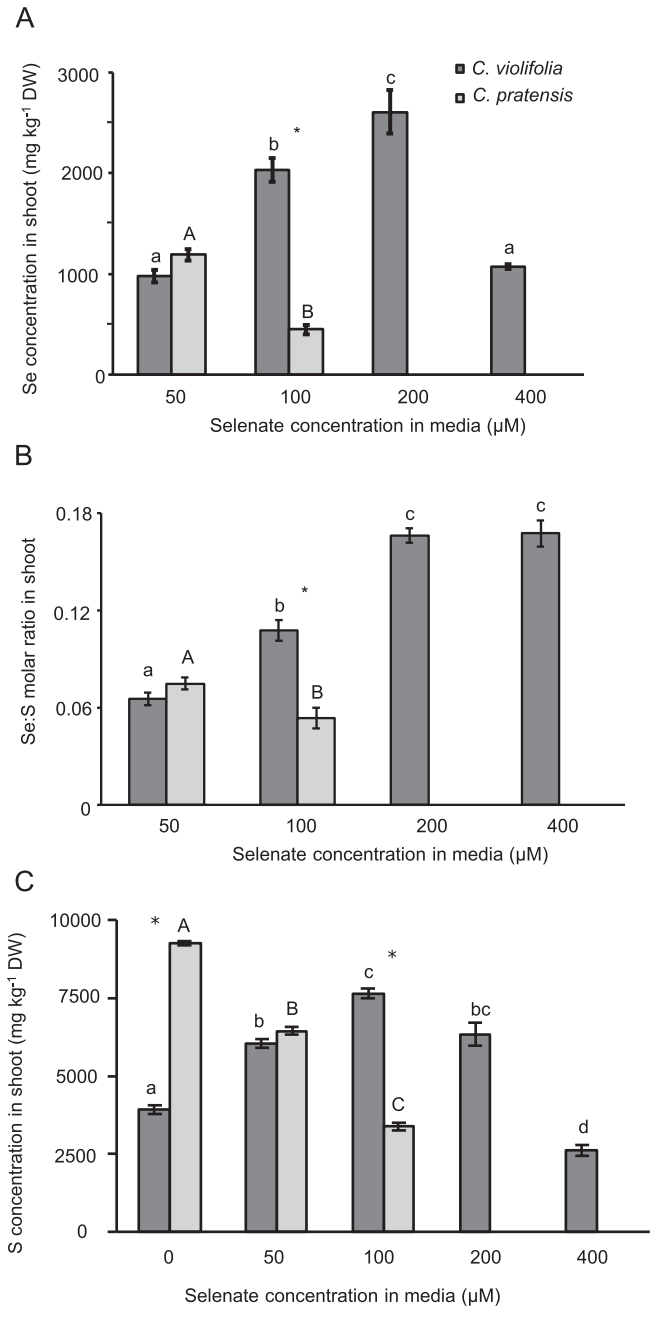

Fig. 2. Selenium concentration (A), Se:S molar ratio (B) and S concentration (C) in shoots of *C. violifolia* and *C. pratensis* grown on agar media supplied with different concentrations of Na_2SeO_4. Values shown are the means ± SEM. Different letters indicate statistically different means among treatments within species, and asterisks indicate statistically different means between species within treatment ($P < 0.05$).

When supplied with 20 μM selenate at the 4-week stage grown on Turface® gravel, both *Cardamine* species accumulated Se to around 400 mg Se/kg DW in their shoot (Fig. 3A). Selenate uptake was equally inhibited in both species (~5-fold) by raising the concentration of the competing ion sulfate 20-fold (Fig. 3A). Shoot Se accumulation from selenite (supplied at 20 μM) was significantly (~2-fold) higher for HA *C. violifolia*; phosphate did not inhibit selenite uptake in either species (Fig. 3A). Shoot Se accumulation from selenite was ~ 10-fold lower than from selenate for both species (Fig. 3A). The shoot:root Se concentration ratio differed between the two species in some respects (Fig. 3C). For plants treated with selenate plus sulfate, this ratio was higher for *C. pratensis* than for *C. violifolia* because root Se level was higher in the HA; no such difference was observed when only selenate was supplied (Fig. 3B). After both selenite treatments (with or without phosphate) the shoot:root Se concentration ratio was 2–3 fold higher in *C. violifolia* than in *C. pratensis* (Fig. 3C).

Cardamine violifolia generally showed higher Se:S ratio in their shoots than *C. pratensis* (Fig. 3F) while *C. pratensis* had higher Se:S ratio in roots (Fig. 3G), indicative of relatively more translocation of Se than S in the HA, as compared to the non-HA. The Se:S ratio was ~1.5-fold and ~2-fold higher in *C. pratensis* and in *C. violifolia* shoots, respectively, compared to that in the medium, when treated with 20 μM selenate (0.08 Se:S molar ratio in the treatment solution; 1/4th Hoagland's solution contains 250 μM sulfate). The Se:S ratio in the shoot was ~ 70% compared to that in the medium when the plants were supplied with 20 μM selenate + 5 mM sulfate (20-fold lower Se:S ratio in the treatment solution).

3.2. Fluorescence and antioxidant capacity analyses

The Chl fluorescence data (Fig. S1) of the two plant species differed significantly for only one parameter: *C. violifolia* had lower relative Chl content for the selenate treatment, compared to *C. pratensis*. The overall pattern was for *C. violifolia* to show less relative chlorophyll and higher NPQt (non-photochemical quenching) than *C. pratensis*, but this was not significant except for the case mentioned. Among treatments and within species, there was one significant treatment effect, only for *C. violifolia*: the selenite plus phosphate treatment had higher NPQt and lower Phi2 (photochemical quenching) compared to selenite alone or control treatments.

The presence of selenate in the media did not have any significant effect on total phenolic content or total antioxidant activity of *C. violifolia* or *C. pratensis* seedlings supplied with or without 25 μM selenate (Table S1). The two species showed a difference in total phenolic content, with *C. pratensis* having ~30% higher levels.

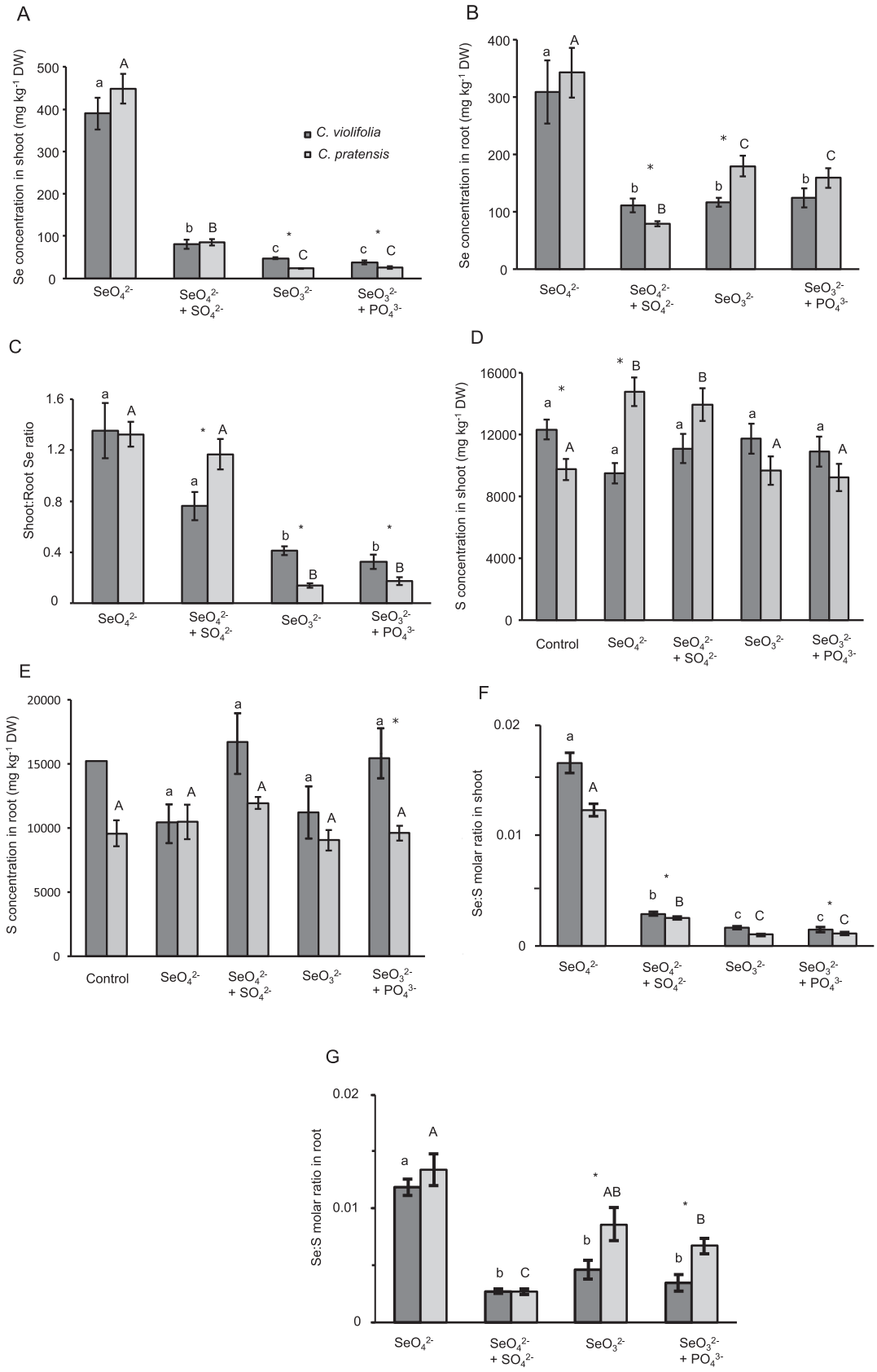

Fig. 3. Selenium concentration in shoots (A) in roots (B), the shoot:root Se ratio (C), S concentration in shoots (D), in roots (E) and Se:S molar ratio in shoots (F) and in roots (G) of *C. violifolia* and *C. pratensis* grown on Turface® gravel media subjected to different treatments: control treatment 1/4th strength Hoagland's solution, 1/4th strength Hoagland's solution with 20 μM Na_2SeO_4, 1/4th strength Hoagland's solution with 20 μM Na_2SeO_4 and 5 mM $MgSO_4$, 1/4th strength Hoagland's solution with 20 μM Na_2SeO_3, 1/4th strength Hoagland's solution with 20 μM Na_2SeO_3 and 2.4 mM KH_2PO_4. In the case of the control treatment, Se concentrations were below LOQ and in case of *C. violifolia* the root dry material was not enough for more replicates and was excluded from statistical evaluation. Values shown are the means ± SEM. Different letters indicate statistically different means among treatments within species, and asterisks indicate statistically different means between species within treatment ($P < 0.05$).

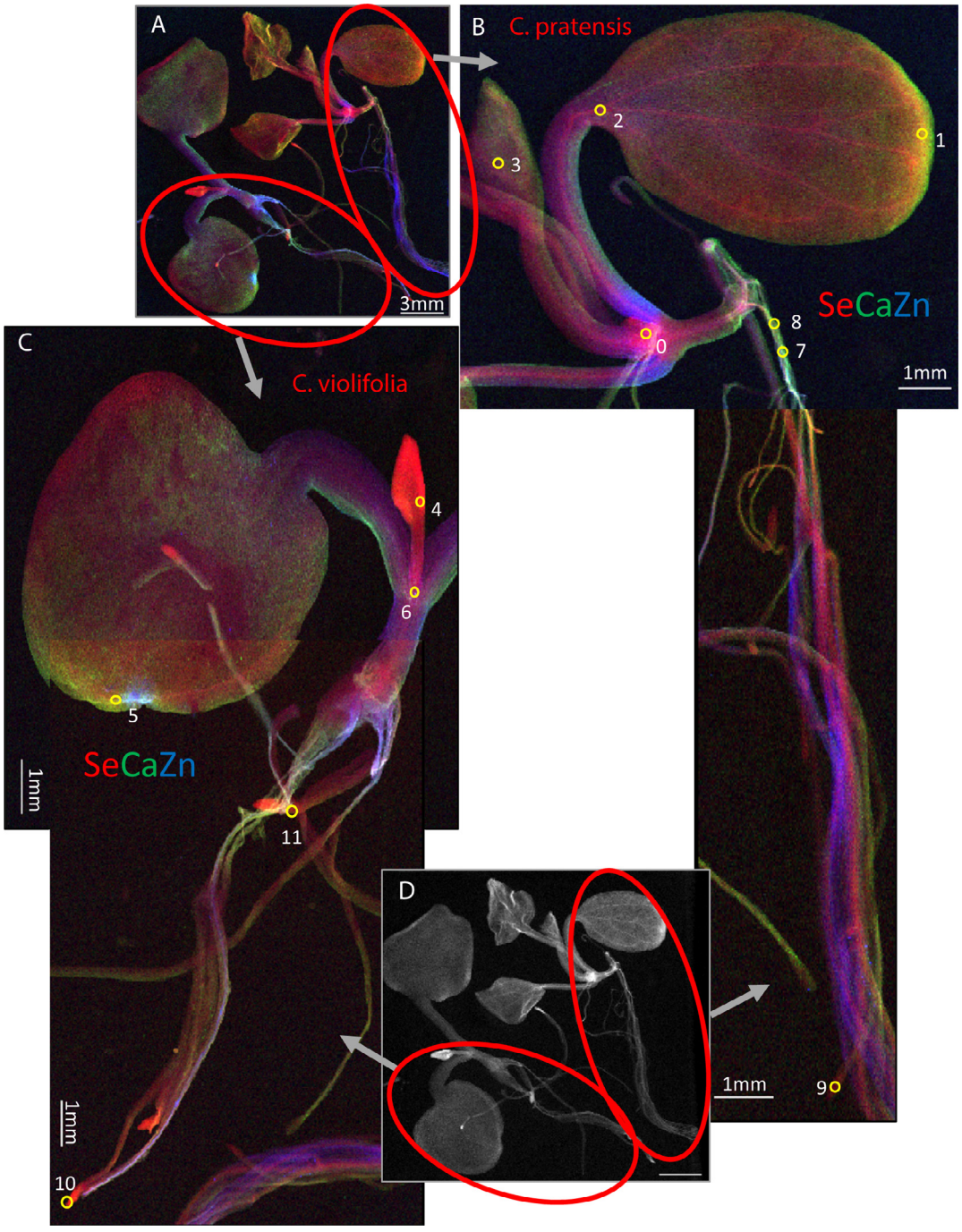

Fig. 4. Micro focused X-ray fluorescence (XRF) elemental maps of seedlings from *C. violifolia* (A, C, D) and *C. pratensis* (A, B, D) grown on agar media supplied with 25 μM selenate. Selenium is shown in red (or in white, D), calcium in green, zinc in blue. Yellow circles denote locations where XANES spectra were collected to determine Se speciation.

Table 1
Selenium speciation in *C. violifolia* (C. v.) and *C. pratensis* (C. p.) as determined by XANES LSQ fitting. Values show the average of the XANES spectra within species and organ, for each of two experimental setups. Corresponding XRF images for agar-grown plants are shown in Fig. 4; gravel-grown XRF images are shown in Fig. 6. Numbers for each form of Se represent the percentage of total Se. ND: not detected. Note that C-Se-C may include selenomethionine, Se-methylselenocysteine, gamma-Glu-Se-methylselenocysteine and selenolanthionine among others.

Organ	Species	Growth media	Supplied Se form	Se(VI) (%)	Se(IV) (%)	C-Se-C (%)	Se(0) (%)	$Se(GSH)_2$ (%)	$SeCys_2$ (%)
Leaf	*C. v.*	gravel	SeO_3	ND	6	91	ND	4	ND
Leaf	*C. v.*	gravel	SeO_4	1	ND	87	ND	4.5	12
Leaf	*C. p.*	gravel	SeO_4	44	ND	59	ND	0	ND
Shoot	*C. v.*	agar	SeO_4	2	4	86	5	4	ND
Shoot	*C. p.*	agar	SeO_4	8	6	84	ND	2	ND
Root	*C. v.*	agar	SeO_4	2	ND	96	ND	1	ND

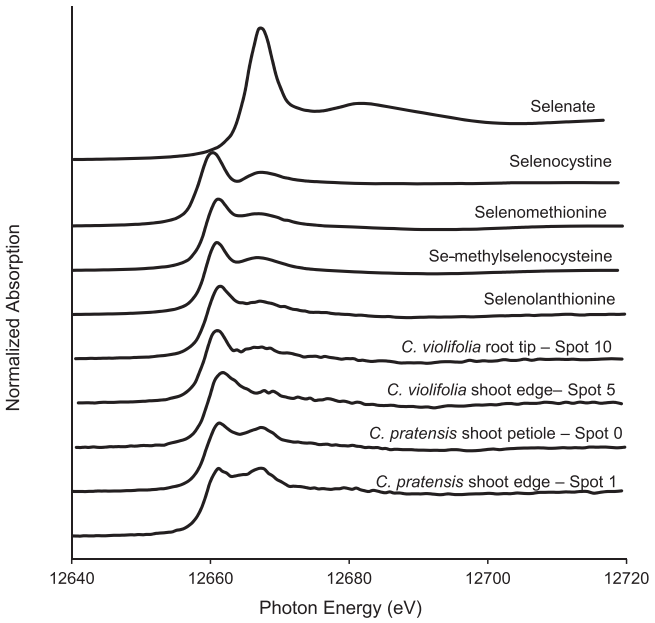

Fig. 5. μXANES spectra of selenium standards (sodium selenate, selenocystine, selenomethionine, Se-methylselenocysteine, selenolanthionine) and *C. violifolia* and *C. pratensis* seedlings (spots denoted in Fig. 4).

3.3. Synchrotron based XRF and XANES experiments

X-ray microprobe analysis on seedlings supplied with selenate showed some differences between the two species in terms of Se localization (Fig. 4). The HA *C. violifolia* showed a pronounced concentration of Se in the tips of the shoot and roots, at the apical meristems, while the non-HA, *C. pratensis*, tended to concentrate Se in its vasculature. The chemical speciation of the Se was indistinguishable for both species by XANES (Table 1): both accumulated predominantly (85%) organic Se with a C-Se-C configuration in their shoot, indistinguishable from selenomethionine, Se-methylselenocysteine or selenolanthionine (Fig. 5). In the root of *C. violifolia* almost all Se was in this form; incidentally, for *C. pratensis* root the XANES Se spectra were of insufficient quality for fitting, due to lower Se signal intensity.

Leaves of the 4-week old Turface® grown *C. violifolia* and *C. pratensis* plants were also analyzed by X-ray microprobe analysis (Fig. 6). At this stage of development, there was a difference in Se speciation between the two species: *C. violifolia* contained ~90% "C-Se-C" compounds, while *C. pratensis* only contained 56% "C-Se-C" and 44% selenate, i.e., the form of Se supplied. The Se distribution was also somewhat different: *C. violifolia* showed a more pronounced Se signal along its leaf edges and in undefined discrete locations along the outside of the petiole; both species also showed slight concentration of Se in the vasculature. When treated with selenite, *C. violifolia* accumulated about 90% of Se in organic "C-Se-C" compounds (Table 1). No adequate Se XANES signal could be obtained from selenite-supplied *C. pratensis*.

3.4. SCX-ICP-MS analyses

Total Se content of *C. violifolia* root and leaf samples collected in the Yutangba region were found to be 157 mg/kg and 261 mg/kg DW, respectively. The strong cation exchange (SCX) chromatography of their water extracts are shown in Fig. 7A and C, respectively. The highest peaks eluting at 3 min were identified in our previous study (Both et al., 2018) as selenolanthionine. Both leaf and root extracts were spiked to 200 ng/ml selenocystine concentration (Fig. 7B and D). The peak of selenocystine eluted at 3.5 min between two peaks originating from the samples, which indicated no selenocystine was present in considerable amount in the water extracts of the leaf and of the root.

Total Se content of *C. pratensis* sample cultivated for LC-ICP-MS analysis was found to be 324 mg/kg DW. The SCX chromatography of leaf water extract is shown in Fig. 8. Inorganic and other anionic Se species are eluting in the void volume at retention time 1.1 min, while several low intensity Se compounds were eluted later. The peaks eluting at 4.6 min and 7.2 min matched the retention times of Se-methylselenocysteine and selenolanthionine, respectively, but their intensity was too low for reliable identification. The extract was spiked with selenocystine in order to check whether the most abundant organic Se compound eluting at 12.1 min might be considered this selenoamino acid dimer; however, the spiking procedure resulted in a separate peak at 11.9 min, indicating no selenocystine was present originally in the leaf water extract in considerable amount.

4. Discussion

At the seedling level, HA *C. violifolia* is clearly more tolerant to selenate than non-HA *C. pratensis* and also accumulated ~3-fold

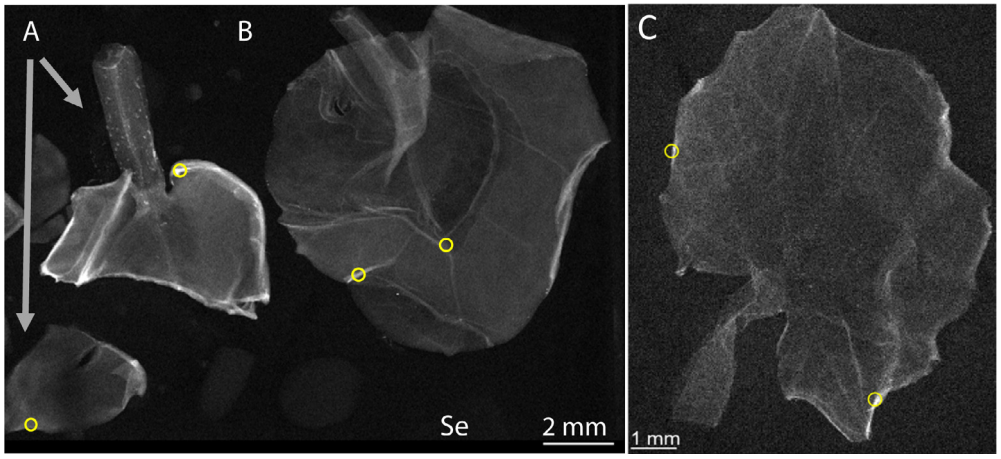

Fig. 6. Micro focused X-ray fluorescence (XRF) elemental maps of leaves from 4-week old *C. violifolia* (A, C) and *C. pratensis* (B) grown on Turface® media supplied with 20 μM selenate (A,B) or selenite (C) for 10 days. Selenium is shown in white. Yellow circles denote locations where XANES spectra were collected to determine Se speciation. Note: *C. pratensis* treated with selenite is not shown for lack of sufficient Se signal. Leaf A broke during transfer of frozen leaf to the XRF cryostage. (For interpretation of the references to colour in this figure legend, the reader is referred to the web version of this article.)

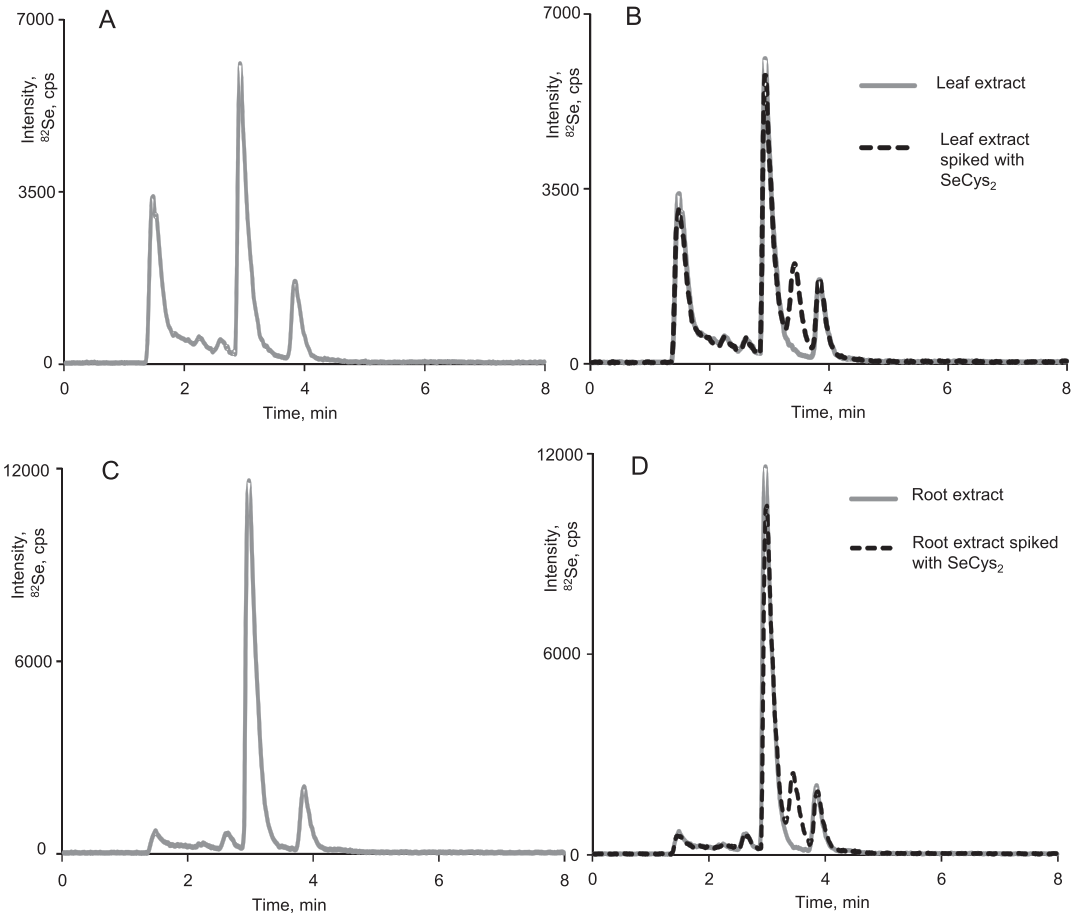

Fig. 7. Strong cation exchange (SCX)-ICP-MS chromatogram of *C. violifolia* leaf (A), root (C) water extract and each spiked to 200 ng/ml selenocystine (dashed line) (B, D).

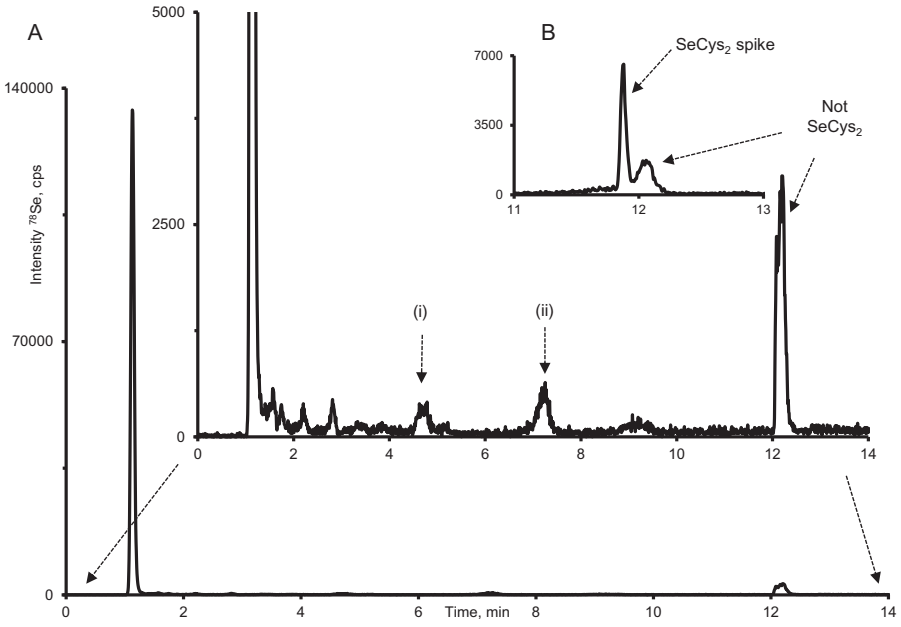

Fig. 8. (A) Strong cation exchange (SCX)-ICP-MS chromatogram of selenium enriched non-HA *C. pratensis* leaf water extract and its spike to 500 ng/ml selenocystine (see the inset (B)). Signs of (i) and (ii) refer to the retention time of Se-methylselenocysteine and selenolanthionine, respectively.

higher Se concentrations in its shoot, upwards of 2000 mg/kg DW without significant toxicity. Neither species showed evidence of growth stimulation by Se at the levels supplied, which is in contrast to Se HA *Symphyotrichum ericoides*, *Astragalus bisulcatus* and *Stanleya pinnata* (El Mehdawi et al., 2012; El Mehdawi et al., 2014). At the highest selenate concentration tested, 400 μM

(32 mg Se/L), *C. violifolia* was still not affected in terms of biomass, but its roots were significantly shorter than the control treatment, likely indicative of toxicity. Thus, there does seem to be a Se tolerance ceiling for the HA. Its shorter roots at 400 μM may in part explain its decreased shoot Se accumulation at that highest concentration. With increasing Se uptake, *C. violifolia* showed increasing S uptake, which is similar to another Se HA, *Astragalus bisulcatus* (El Mehdawi et al., 2014) and to secondary Se accumulator *Brassica juncea* (Harris et al., 2014).

The shoot Se concentration in mature plants was lower than in seedlings, which may be explained by the difference in supplied concentration: shoot Se concentration was 2.5-fold lower in 4-week old plants treated with 20 μM selenate, as compared to in seedlings treated with 50 μM selenate. In addition, there may be a Se dilution effect in mature plants *vs*. seedlings, and it is also possible that the rate of selenate uptake varies across the plant's development. In contrast to the seedling results, the mature plant experiments showed no differences between the species with respect to shoot Se accumulation from selenate. However, *C. violifolia* did show ~2-fold higher Se accumulation than *C. pratensis* from selenite. In both species, shoot Se accumulation was higher from selenate than from selenite, which is consistent with earlier studies, and reflects the different transport mechanisms for these two compounds via sulfate and phosphate transporters, respectively (de Souza et al., 1998). Sulfate inhibited selenate uptake, as expected, since both are taken up by the same group of sulfate transporters (SULTRs) (Schiavon and Pilon-Smits, 2017). The two *Cardamine* species did not show any difference in this respect. This is in contrast to other Se HA such as *S. pinnata*, which have more selenate-specific uptake that is less inhibited by sulfate (El Mehdawi et al., 2018; Harris et al., 2014; White et al., 2007). Contrary to expectations, selenite uptake was not inhibited by phosphate for either of the two *Cardamine* species, and thus it appears that this process is not mediated by phosphate transporters in these plants. The mechanism for selenite uptake in this group will be interesting for further investigation, and may involve anion channels, as reported for some species (Schiavon and Pilon-Smits, 2017).

The shoot Se:S ratio was higher for *C. violifolia* than *C. pratensis*, both when treated with selenate or selenite. This apparent difference in translocation between Se and S in the HA may be caused by a Se-specific root-to-shoot transporter, or may point to translocation of Se and S in different chemical forms that use different transporters (e. g., organic Se *vs.* inorganic S). Some Se HA have shown evidence of enhanced Se assimilation in roots, as judged from molecular/biochemical/physiological data (Wang et al., 2018), and also showed relatively higher Se:S translocation in xylem and phloem (Cappa et al., 2014). The molecular mechanisms for these HA-specific transport mechanisms are currently unknown.

Based on the Chl fluorescence parameters, *C. violifolia* appeared to have overall lower relative chlorophyll content and higher NPQt, compared to *C. pratensis*, regardless of treatment. This may be interpreted to be indicative of less well functioning light reactions, but no sign of enhanced stress is apparent from the other physiological measurements. Perhaps the observed differences are somehow related to the adaptation of *C. violifolia* to high Se soils. Among the treatments, the selenite plus phosphate treatment stood out from the others, with Chl fluorescence parameters indicative of more stress, particularly for *C. violifolia*; there was a similar but non-significant pattern seen for *C. pratensis*. It is possible that the phosphate concentration used (10x higher than normal) caused salinity stress. The observed effects do not seem to be Se-related, because the selenite-only treatment did not show the same effect. Interesting to note is that Zhou et al. (2018) found that high selenite concentration suppressed the expression of photosynthetic genes in *C. hupingshanensis*; however, in that study a 50-fold higher selenite concentration was used than here.

There were clear differences between *C. violifolia* and *C. pratensis* with respect to Se localization and speciation. At the seedling stage, the HA showed a pronounced Se sequestration in its shoot and root apical meristems, while the non-HA accumulated its Se mostly in its vasculature. Also, at the 4-week old stage the HA had more pronounced Se concentration in particular locations in the leaf periphery, while the non-HA only showed some Se concentration in the vasculature. It cannot be excluded that the higher Se signal in the leaf periphery was due to leaf curling, but it was seen only in the HA. In an earlier μ-XRF study, Cui et al. (2018) concluded that in the HA *Cardamine* species Se was primarily located in the cortex, endodermis, and vascular cylinder in roots, while in the epidermis, it was the cortex and vascular bundle of stems and concentrated in the leaf veins and the peripheral parts of leaves. These results agree with our leaf data of *C. violifolia*. Sequestration along the leaf periphery is what was also found for the other HA species *Astragalus bisulcatus* and *Stanleya pinnata* (Freeman et al., 2006). The concentration of Se in the leaf periphery of the HA may be indicative of specialized Se sequestration mechanisms in areas where Se can be tolerated to the highest extent and where it may offer the most ecological benefits via herbivore or pathogen protection. Concentration of Se in the leaf vasculature, as seen particularly in non-HA *C. pratensis*, is similar to what was found in other non-HA *Brassicaceae* such as *Brassica juncea* (Freeman et al., 2006); it may reflect a more limiting uptake rate from the xylem into the mesophyll cells.

The two *Cardamine* species differed in Se speciation, when sampled at the mature plant stage. The main form(s) of Se in the HA *C. violifolia* had "C-Se-C" configuration, while the non-HA had relatively more selenate. This difference in speciation was not apparent at the seedling level, where both species contained "C-Se-C". It is possible that the relative enzyme activities differ with developmental stage, or that the differences in selenate supply affected the speciation outcome. The finding that at the mature plant stage the main form(s) of Se in the HA *C. violifolia* had "C-Se-C" configuration, while the non-HA had relatively more selenate shows parallels to earlier studies comparing *S. pinnata* and *A. bisulcatus* with non-HA relatives (Alford et al., 2014; Freeman et al., 2006). The presence of relatively more organic Se suggests that the HA has a more active sulfate/selenate assimilation pathway, converting selenate to organic "C-Se-C" forms. The form of Se in the different HA, although all "C-Se-C", may differ: *A. bisulcatus* and *S. pinnata* were found using LC-MS to contain mostly Se-methylselenocysteine, and *S. pinnata* also contains selenocystathionine. The XANES data collected here identify the Se in *C. violifolia* also as "C-Se-C", in agreement with our earlier selenolanthionine identification using LC-ICP-MS and LC-ESI-MS, which was further supported by chemical synthesis (Both et al., 2018). Results of μ-XANES experiments by Cui et al. (2018) on HA *Cardamine* found the majority of Se to be in the form of "C-Se-C" compounds in roots and stems, but leaves were shown to contain the "C-Se$^-$" form of Se, using selenocystine as model compound. According to Table 1, LSQ fitting also indicated 12% of Se in the form of "C-Se-Se-C" in the leaf of *C. violifolia* grown on gravel medium with selenate supplementation. Therefore, carrying out the SCX-ICP-MS analyses to determine whether selenocystine might be responsible for this result was highly required. On the other hand, the lack of selenocystine in the water extracts doesn't exclude the possible presence of minor water soluble "C-Se-Se-C" species such as selenohomocystine and its derivatives (Németh et al., 2013) or even some plant proteins (Cheajesadagul et al., 2014) where inherent "S(e)-S(e)" bonds can be present (e.g., like in the granule-bound starch synthase in rice; Uniprot entry Q0DEV5). In any case, selenocystine accumulation cannot be regarded considerable in *C. violifolia*.

It is of note that several conflicting LC-based chemical speciation reports have been published for *Cardamine* (Both et al., 2018; Cui et al., 2018; Yuan et al., 2013). Comparison of these Se speciation data is complicated by the fact that the different chromatographic approaches did not include comparable Se species assignment procedures, especially concerning selenocystine. Our result calls attention to the careful selection of chromatographic setups in order to provide an adequate level of species assignment: indeed, at least two independent separation mechanisms are required for the verification of a Se species, and even one mismatch is enough for declining a candidate analyte (Francesconi and Sperling, 2005).

5. Conclusions

This comparative study has revealed basic differences between HA and non-HA *Cardamine* species with respect to Se tolerance, Se accumulation and partitioning, as well as in Se localization and speciation. Together, these have given new insight into physiological and biochemical hyperaccumulation mechanisms. The results from *C. violifolia* contrast in some respects with other Se HA such as *A. bisulcatus* and *S. pinnata*, such as absence of growth stimulation by Se and the presence of sulfate-mediated inhibition of selenate uptake. Still more studies are warranted to fully understand the mechanisms underlying Se hyperaccumulation in *C. violifolia* because according to the information so far *C. violifolia* doesn't fit into the previously described classes of primary and secondary Se accumulator plants.

Declaration of Competing Interest

The authors declare that they have no known competing financial interests or personal relationships that could have appeared to influence the work reported in this paper.

Acknowledgements

E. B. Both acknowledges scholarship of Campus Mundi Program (EFOP-3.4.2-VEKOP-15-2015-00001) and support of Doctoral School of Food Sciences, Szent István University, Hungary. J. Xiang and H. Yin acknowledge the support from the National Natural Science Foundation of China (NNSFC; project code 3156110472, Physiological and genetic mechanisms of *Cardamine violifolia* E. Schulz of selenium tolerance and hyperaccumulation in Enshi, China). M. Dernovics acknowledges Bolyai János Research Scholarship of the Hungarian Academy of Sciences (Hungarian Academy of Sciences). A. Wangeline acknowledges support from an Institutional Development Award (IDeA) from the National Institute of General Medical Sciences of the National Institutes of Health under Grant # 2P20GM103432. E.A.H. Pilon-Smits acknowledges financial support from National Science Foundation grant IOS-1456361. This research used resources of the Advanced Light Source, which is a DOE Office of Science User Facility under contract no. DE-AC02-05CH11231.

Appendix A. Supplementary data

Supplementary data to this article can be found online at https://doi.org/10.1016/j.scitotenv.2019.135041.

References

Alford, E.R., Lindblom, S.D., Pittarello, M., Freeman, J.L., Fakra, S.C., Marcus, M.A., et al., 2014. Roles of rhizobial symbionts in selenium hyperaccumulation in astragalus (Fabaceae). Am. J. Bot. 101, 1895–1905.

Banuelos, G.S., Fakra, S.C., Walse, S.S., Marcus, M.A., Yang, S.I., Pickering, I.J., et al., 2011. Selenium accumulation, distribution, and speciation in spineless prickly pear cactus: a drought- and salt-tolerant, selenium-enriched nutraceutical fruit crop for biofortified foods. Plant Physiol. 155, 315–327.

Both, E.B., Shao, S.X., Xiang, J.Q., Jokai, Z., Yin, H.Q., Liu, Y.F., et al., 2018. Selenolanthionine is the major water-soluble selenium compound in the selenium tolerant plant Cardamine violifolia. Biochim. Biophys. Acta Gen. Subj. 1862, 2354–2362.

Cappa, J.J., Cappa, P.J., El Mehdawi, A.F., McAleer, J.M., Simmons, M.P., Pilon-Smits, E.A.H., 2014. Characterization of selenium and sulfur accumulation across the genus Stanleya (Brassicaceae): a field survey and common-garden experiment. Am. J. Bot. 101, 830–839.

Chang, C.Y., Yin, R.S., Wang, X., Shao, S.X., Chen, C.Y., Zhang, H., 2019. Selenium translocation in the soil-rice system in the Enshi seleniferous area, Central China. Sci. Total Environ. 669, 83–90.

Cheajesadagul, P., Bianga, J., Arnaudguilhem, C., Lobinski, R., Szpunar, J., 2014. Large-scale speciation of selenium in rice proteins using ICP-MS assisted electrospray MS/MS proteomics. Metallomics 6, 646–653.

Crecelius, A.C., Holscher, D., Hoffmann, T., Schneider, B., Fischer, T.C., Hanke, M.V., et al., 2017. Spatial and temporal localization of flavonoid metabolites in strawberry fruit (Fragaria × ananassa). J. Agric. Food. Chem. 65, 3559–3568.

Cruz-Jimenez, G., Peralta-Videa, J.R., de la Rosa, G., Meitzner, G., Parsons, J.G., Gardea-Torresdey, J.L., 2005. Effect of sulfate on selenium uptake and chemical speciation in Convolvulus arvensis L. Environ. Chem. 2, 100–107.

Cui, L.W., Zhao, J.T., Chen, J.Y., Zhang, W., Gao, Y.X., Li, B., et al., 2018. Translocation and transformation of selenium in hyperaccumulator plant Cardamine enshiensis from Enshi, Hubei, China. Plant Soil 425, 577–588.

de Souza, M.P., Pilon-Smits, E.A.H., Lytle, C.M., Hwang, S., Tai, J., Honma, T.S.U., et al., 1998. Rate-limiting steps in selenium assimilation and volatilization by Indian mustard. Plant Physiol. 117, 1487–1494.

Eiche, E., Bardelli, F., Nothstein, A.K., Charlet, L., Gottlicher, J., Steininger, R., et al., 2015. Selenium distribution and speciation in plant parts of wheat (Triticum aestivum) and Indian mustard (Brassica juncea) from a seleniferous area of Punjab, India. Sci. Total Environ. 505, 952–961.

El Mehdawi, A.F., Cappa, J., Fakra, S., Self, J., Pilon-Smits, E., 2012. Interactions of selenium hyperaccumulators and nonaccumulators during cocultivation on seleniferous or nonseleniferous soil–the importance of having good neighbors. New Phytol. 194, 264–277.

El Mehdawi, A.F., Jiang, Y., Guignardi, Z.S., Esmat, A., Pilon, M., Pilon-Smits, E.A.H., et al., 2018. Influence of sulfate supply on selenium uptake dynamics and expression of sulfate/selenate transporters in selenium hyperaccumulator and nonhyperaccumulator Brassicaceae. New Phytol. 217, 194–205.

El Mehdawi, A.F., Reynolds, R.J.B., Prins, C.N., Lindblom, S.D., Cappa, J.J., Fakra, S.C., et al., 2014. Analysis of selenium accumulation, speciation and tolerance of potential selenium hyperaccumulator Symphyotrichum ericoides. Physiol. Plant. 152, 70–83.

Fakra, S.C., Luef, B., Castelle, C.J., Mullin, S.W., Williams, K.H., Marcus, M.A., et al., 2018. Correlative cryogenic spectromicroscopy to investigate selenium bioreduction products. Environ. Sci. Technol. 52, 503–512.

Fassel, V.A., 1978. Quantitative elemental analyses by plasma emission-spectroscopy. Science 202, 183–191.

Fordyce, F.M., Zhang, G.D., Green, K., Liu, X.P., 2000. Soil, grain and water chemistry in relation to human selenium-responsive diseases in Enshi District China. Appl. Geochem. 15, 117–132.

Francesconi, K.A., Sperling, M., 2005. Speciation analysis with HPLC-mass spectrometry: time to take stock. Analyst 130, 998–1001.

Freeman, J.L., Marcus, M.A., Fakra, S.C., Devonshire, J., McGrath, S.P., Quinn, C.F., et al., 2012. Selenium hyperaccumulator plants Stanleya pinnata and Astragalus bisulcatus are colonized by Se-resistant, Se-excluding wasp and beetle seed herbivores. PLoS ONE 7, 50516.

Freeman, J.L., Tamaoki, M., Stushnoff, C., Quinn, C.F., Cappa, J.J., Devonshire, J., et al., 2010. Molecular mechanisms of selenium tolerance and hyperaccumulation in Stanleya pinnata. Plant Physiol. 153, 1630–1652.

Freeman, J.L., Zhang, L.H., Marcus, M.A., Fakra, S., McGrath, S.P., Pilon-Smits, E.A.H., 2006. Spatial imaging, speciation, and quantification of selenium in the hyperaccumulator plants Astragalus bisulcatus and Stanleya pinnata. Plant Physiol. 142, 124–134.

Games, P.A., Howell, J.F., 1976. Pairwise multiple comparison procedures with unequal N's and/or variances: a Monte Carlo study. J. Educat. Statist. 1, 113–125.

Harris, J., Schneberg, K.A., Pilon-Smits, E.A.H., 2014. Sulfur-selenium-molybdenum interactions distinguish selenium hyperaccumulator Stanleya pinnata from non-hyperaccumulator Brassica juncea (Brassicaceae). Planta 239, 479–491.

Hoagland, D.R., Arnon, D.I., 1950. The water-culture method for growing plants without soil. Circ. Calif. Agricult. Exp. Station 347, 32 pp.

Jaccard, J., Becker, M.A., Wood, G., 1984. Pairwise multiple comparison procedures – a review. Psychol. Bull. 96, 589–596.

Jiang, Y., El Mehdawi, A.F., Tripti, Lima LW, Stonehouse, G., Fakra, S.C., et al., 2018. Characterization of selenium accumulation, localization and speciation in buckwheat-implications for biofortification. Front. Plant Sci. 871, 1583.

Lindblom, S.D., Fakra, S.C., Landon, J., Schulz, P., Tracy, B., Pilon-Smits, E.A.H., 2014. Inoculation of selenium hyperaccumulator Stanleya pinnata and related non-accumulator Stanleya elata with hyperaccumulator rhizosphere fungi – investigation of effects on Se accumulation and speciation. Physiol. Plant. 150, 107–118.

Miller, N.J., Rice-Evans, C.A., 1996. Spectrophotometric determination of antioxidant activity. Redox Rep. 2, 161–171.
Montes-Bayon, M., Yanes, E.G., de Leon, C.P., Jayasimhulu, K., Stalcup, A., Shann, J., et al., 2002. Initial studies of selenium speciation in Brassica juncea by LC with ICPMS and ES-MS detection: an approach for phytoremediation studies. Anal. Chem. 74, 107–113.
Murashige, T., Skoog, F., 1962. A Revised Medium for Rapid Growth and Bio Assays with Tobacco Tissue Cultures. Physiol. Plantarum 15, 473–497.
Németh, A., García Reyes, J.F., Kosáry, J., Dernovics, M., 2013. The relationship of selenium tolerance and speciation in Lecythidaceae species. Metallomics 5, 1663–1673.
Ogra, Y., Kitaguchi, T., Ishiwata, K., Suzuki, N., Iwashita, Y., Suzuki, K.T., 2007. Identification of selenohomolanthionine in selenium-enriched Japanese pungent radish. J. Anal. At. Spectrom. 22, 1390–1396.
Qin, H.B., Zhu, J.M., Su, H., 2012. Selenium fractions in organic matter from Se-rich soils and weathered stone coal in selenosis areas of China. Chemosphere 86, 626–633.
Rueden, C.T., Schindelin, J., Hiner, M.C., DeZonia, B.E., Walter, A.E., Arena, E.T., et al., 2017. Image J2: ImageJ for the next generation of scientific image data. BMC Bioinformatics 18, 529.
Sarabia, L.D., Boughton, B.A., Rupasinghe, T., van de Meene, A.M.L., Callahan, D.L., Hill, C.B., et al., 2018. High-mass-resolution MALDI mass spectrometry imaging reveals detailed spatial distribution of metabolites and lipids in roots of barley seedlings in response to salinity stress. Metabolomics 14, 63.
Schiavon, M., Pilon-Smits, E.A.H., 2017. The fascinating facets of plant selenium accumulation – biochemistry, physiology, evolution and ecology. New Phytol. 213, 1582–1596.
Shao, S.X., Deng, G.D., Mi, X.B., Long, S.Q., Zhang, J., Tang, J., 2014. Accumulation and speciation of selenium in Cardamine sp. in Yutangba Se Mining Field, Enshi, China. Chin. J. Geochem. 33, 357–364.
Silva, V.M., Boleta, E.H.M., Lanza, M., Lavres, J., Martins, J.T., Santos, E.F., et al., 2018. Physiological, biochemical, and ultrastructural characterization of selenium toxicity in cowpea plants. Environ. Exp. Bot. 150, 172–182.
Singleton, V.L., Rossi, J.A., 1965. Colorimetry of total phenolics with phosphomolybdic-phosphotungstic acid reagents. Am. J. Enol. Viticult. 16, 144–158.
Sors, T.G., Martin, C.P., Salt, D.E., 2009. Characterization of selenocysteine methyltransferases from Astragalus species with contrasting selenium accumulation capacity. Plant J. 59, 110–122.
Statwick, J., Majestic, B.J., Sher, A.A., 2016. Characterization and benefits of selenium uptake by an Astragalus hyperaccumulator and a non-accumulator. Plant Soil 404, 345–359.
Tukey, J.W., 1977. Exploratory Data Analysis. Addison-Wesley Publishing Company, Reading, MA.
Virupaksha, T.K., Shrift, A., 1963. Biosynthesis of selenocystathionine from selenate in Stanleya pinnata. BBA 74, 791–793.
Wang, J.M., Cappa, J.J., Harris, J.P., Edger, P.P., Zhou, W., Pires, J.C., et al., 2018. Transcriptome-wide comparison of selenium hyperaccumulator and nonaccumulator Stanleya species provides new insight into key processes mediating the hyperaccumulation syndrome. Plant Biotechnol. J. 16, 1582–1594.
White, P.J., Bowen, H.C., Marshall, B., Broadley, M.R., 2007. Extraordinarily high leaf selenium to sulfur ratios define 'Se-accumulator' plants. Ann. Bot. 100, 111–118.
Xing, K., Zhou, S.B., Wu, X.G., Zhu, Y.Y., Kong, J.J., Shao, T., et al., 2015. Concentrations and characteristics of selenium in soil samples from Dashan Region, a selenium-enriched area in China. Soil Sci. Plant Nutr. 61, 889–897.
Yuan, L.X., Zhu, Y.Y., Lin, Z.Q., Banuelos, G., Li, W., Yin, X.B., 2013. A Novel selenocystine-accumulating plant in selenium-mine drainage area in Enshi, China. Plos One 8, 2789.
Zarcinas, B.A., Cartwright, B., Spouncer, L.R., 1987. Nitric-acid digestion and multielement analysis of plant-material by inductively coupled plasma spectrometry. Commun. Soil Sci. Plant Anal. 18, 131–146.
Zhou, Y.F., Tang, Q.Y., Wu, M.R., Mou, D., Liu, H., Wang, S.C., et al., 2018. Comparative transcriptomics provides novel insights into the mechanisms of selenium tolerance in the hyperaccumulator plant Cardamine hupingshanensis. Sci. Rep. 8, 17.
Zhu, J.M., Wang, N., Li, S., Li, L., Su, H., Liu, C.X., 2008. Distribution and transport of selenium in Yutangba, China: impact of human activities. Sci. Total Environ. 392, 252–261.
Zhu, J.M., Zuo, W., Liang, X.B., Li, S.H., Zheng, B.S., 2004. Occurrence of native selenium in Yutangba and its environmental implications. Appl. Geochem. 19, 461–467.